Cooperative Integration of Harvesting RF Sections for Passive RFID Communication

Gianfranco Andía Vera, Dahmane Allane, Apostolos Georgiadis, *Senior Member, IEEE*, Ana Collado, *Senior Member, IEEE,* Yvan Duroc, Smail Tedjini, *Senior Member, IEEE*

***Abstract*—This paper proposes a novel cooperative composite energy harvesting system that consists in the association of a traditional passive UHF Radio Frequency Identification (RFID) chip with an Electromagnetic Energy Harvesting Circuit (EEH-C). The objective is to exploit the i-v nonlinearity of the rectifier by applying a signal with time-varying envelope in order to improve the RF-to-dc conversion efficiency. Thanks to a multisource configuration, i.e. an RFID reader at 0.868 GHz and an external source at 2.45 GHz, the EEH-C is able to rectify the 3rd harmonic product of the RFID chip, in addition to the 2.45 GHz signal, without compromising the RFID communication. Additionally, digitally modulated signals are used at 2.45 GHz to further enhance the harvesting efficiency of the EEH-C. From theory, simulations and measurement it is demonstrated that the exploitation of the three nonlinear effects of rectifying circuits, i.e., (i) impedance power dependency, (ii) harmonic signals production, and (iii) waveform dependency can greatly improve the conversion efficiency of the EEH-C.**

***Index Terms*— Energy harvesting, non-linearity, harmonic balance, RFID, UHF passive tags, wireless power transmission.**

I. Introduction

RADIO Frequency Identification (RFID) is a wireless data-collection technology very popular in different applications and services such as logistics, manufacturing, access control and security. Sixty years after the publication of its principle of operation [1], the RFID technology continues being part of the « top ten » technologies worldwide. The scope of the RFID technology is nowadays not only limited to the identification and tracking of inventory, but it is capable to collect and compile massive amounts of detailed real-time data in different types of environments around us. Therefore the evolution of RFID opens the way for a plethora of new applications in the area of Internet of Things (with 50 billion connected objects expected for 2020), Smart Skins, Man-to-Machine and Cognitive Intelligence [2].

This growing interest is primarily related to the significant benefits of passive Ultra High Frequency (UHF) RFID, in particular, its passive and wireless features that provide decisive practical advantages. For passive UHF RFID tags the reader transfers energy wirelessly to the tag by sending Radio Frequency (RF) power (at 868 MHz in Europe and in 902-926 MHz band in US) that the tag must collect and transform into dc power to operate and respond using the backscattering modulation technique [3]. Consequently the passive RFID technology naturally embeds the principle of Wireless Power Transmission (WPT) using an intentional Electromagnetic (EM) source.

However the requirement of additional functions for smart tags has strongly raised the need of additional sources of energy [4]. The idea of the tag-sensor approach is to associate new sensing capabilities to the tag while it is still enjoying the identification functionality and all this in a wireless environment. Many studies have demonstrated the possibilities of this concept in different contexts, e.g. for industrial or urban areas, agricultural zones, or Body Area Networks (BAN). A wide variety of sensor capabilities have been also shown: temperature, pressure, humidity, deformation, crack width, accelerometer, chemical sensors, etc. Two types of implementations are used where either the tag integrates the sensor or the sensor function is integrated in the tag [5]. In the first case, the difficulties reside in the supply autonomously the sensor via the rectifier circuit of the tag itself (very constraint solution) or via another energy recovery circuit. Among the possible energy sources, the natural or ecologic sources such as solar, thermal, kinetic are of first interest. However and always with an ecofriendly regard, the presented work only focuses on the EM sources and proposes a new and original cooperative powering system that exploits wasted EM energies. The approach consists in the association of a traditional passive UHF RFID tag with an Electromagnetic Energy Harvesting Circuit (EEH-C) that efficiently performs

Manuscript received July 1, 2015. This paper is an expanded paper from the IEEE MTT-S International Microwave Symposium, Phoenix, AZ, USA, May 18–22, 2015. This work was supported by the EU COST Action IC1301 "Wireless Power Transmission for Sustainable Electronics" (WIPE). The work of A. Georgiadis and A. Collado was funded by the Spanish MEC and FEDER funds through project TEC2012-39143 and the Generalitat de Catalunya under grant 2014 SGR 1551.

G. Andia Vera, D. Allane, and S. Tedjini are with the Laboratoire de Conception et d'Intégration des Systèmes (LCIS), Grenoble Institute of Technology (Grenoble INP), 26902 Valence, France (e-mail: gianfranco.andia-vera@lcis.grenoble-inp.fr; dahmane.allane@lcis.grenoble-inp.fr; smail.tedjini@grenoble-inp.fr).

Y. Duroc is with Ampere Lab, Lyon University, 43 boulevard du 11 novembre 1918, 69622 Villeurbanne, France (e-mail: yvan.duroc@univ-lyon1.fr).

A. Georgiadis and A. Collado are with the Centre Tecnologic de Telecomunicacions de Catalunya (CTTC), 08860 Castelldefels, Spain (e-mail: ageorgiadis@cttc.es; acollado@cttc.es).

Color versions of one or more of the figures in this paper are available online at http://ieeexplore.ieee.org.

Digital Object Identifier 00.0000/TMTT.2015.0000000

RF-to-dc conversion from an RF source at 2.45 GHz combined with the 3rd harmonic product generated by the chip (so-called $3f_{0chip}$). Contrary to some works in the literature that present a cooperative harvesting operation by adding the dc outputs of different harvesters, i.e. at dc level [6]-[7], It is worth noting that the cooperation proposed in this approach is done at RF level, i.e., it is based on the co-existence and mutual cooperation of two RF systems (EEH-C and RFID chip) without compromising the communication function.

The proposed study covers all the aspects from theory, simulation and experimental results in order to highlight the three nonlinear effects of rectifying circuits exploited with mutual benefits: (i) impedance power dependency [8], (ii) harmonic signals production [9], and (iii) waveform dependency [10].

The paper is organized as follows. In Section II, the state-of-art and underpinning theory about the exploitation of the nonlinear i-v characteristic of rectifier circuits used in this composite system are exposed. Section III introduces the original composite harvesting system proposed in this work and explains the design methodology of the system. Section IV presents the results of an in-depth simulation study based on the multisource operation and the $3f_{0chip}$ rectification. In Section V, the approach is validated by means of experimental tests using conducted measurements. Finally Section VI draws the final conclusions and associated perspectives.

II. Review and theory

The proposed work builds on the possibility of enhancing the RF-to-dc conversion efficiency of rectifier circuits by applying a multi-frequency excitation signal. The nonlinear i-v characteristic of rectifier circuits can potentially lead to an enhanced RF-to-dc conversion efficiency when they are excited simultaneously by more than one signal relative to a single Continuous Wave (CW) signal of the same average power, such as the signal provided by the standard RFID reader. This effect was verified experimentally in [11], where the performance of a wideband rectifier was tested using pairs of CW tone signals with different frequencies and power levels. In [12], an improvement in the read range of passive RFID tags of up to 24 % was obtained by interrogating them using multi-tone signals with up to 8 subcarriers which were named power-optimized waveforms.

A composite signal of a number of tones, or alternatively a finite bandwidth signal with arbitrary modulation can be expressed mathematically in a general form as a (multi-harmonic) signal with a time-varying envelope. A time-varying envelope results in the presence of instantaneous power peaks in the signal and a certain Peak-to-Average-Power-Ratio (PAPR). An improvement in the rectifier RF-to-dc conversion efficiency using Quadrature Phase-Shift Keying (QPSK) modulated input signals was reported in [13]. Interest in the potential efficiency improvement by tailoring the transmitted signal envelope properties has spurred a number of subsequent publications studying the effect of efficiency and the PAPR of multi-sine signals [14]-[16], or modulated signals [10],[17] and even white noise and chaotic waveforms [10],[18]. In [19] an efficiency improvement compared to CW signal was demonstrated using a composite 2-tone signal which included two approximately harmonically related tones at 0.810 GHz and 1.580 GHz. In the work presented here, a composite energy harvesting system is considered which includes two rectifier circuits, one operating at the fundamental UHF RFID frequency of 0.868 GHz and a second one operating near its 3rd harmonic. The reason behind the choice of the second operating frequency band is two-fold, first in order to potentially recover energy from generated 3rd harmonic products from the first rectifier circuit, i.e. the RFID chip, and second to harvest energy from digitally modulated signals corresponding to existing ambient transmissions at the 2.4 GHz Industrial Scientific and Medical (ISM) band such as nearby Wi-Fi routers.

It should be emphasized that the efficiency improvement is dependent on the average power of the input signal [10][11][15], since the increased instantaneous peak power may drive the nonlinear rectifying element (e.g. Schottky diode) in its breakdown region which results in increased dissipation losses, or lead to impedance mismatch at the input of the rectifier which results in reflection losses and subsequently a reduction in the obtained efficiency. In summary, the actual improvement in efficiency is a function of the signal properties such as its average power and envelope characteristics like its PAPR, the nonlinear rectifying device i-v characteristic, as well as the input matching network of the rectifier and rectifier load.

III. Composite Energy harvesting system

With the intention to profit from the nonlinear i-v characteristic of rectifier circuits in presence of time-varying envelope signals, a composite signal generated by a composite energy harvesting system (multisource) and $3f_{0chip}$ will be build. This section describes the composite system. The approach of using a finite bandwidth signal with arbitrary modulation will be later exploited (see Section V) using the same composite energy harvesting system.

A. Frequency considerations and power management

In this work, the RFID communication is set to operate with a fixed carrier at 0.868 GHz as per the regulation in Europe, in where the frequency hopping mode is not implemented [20]. A wider bandwidth centered at 2.45 GHz ISM band is also considered. Indeed frequencies from 802.11b/g/n Wi-Fi standards with communications channels located between 2.44 GHz and 2.46 GHz are exploited [21]. It is worth noting that the scope of this work does not consider the harvesting power management but only proposes an innovative cooperative harvesting method. However, some complements on the power management trends in harvesting applications are discussed in the following paragraph.

One point to be considered is that most of the ambient RF power densities to be harvested are very low and the produced energy usually is not enough for most continuous electronic functions. However if this energy is efficiently stored over time, realistic functions can be performed in discrete time

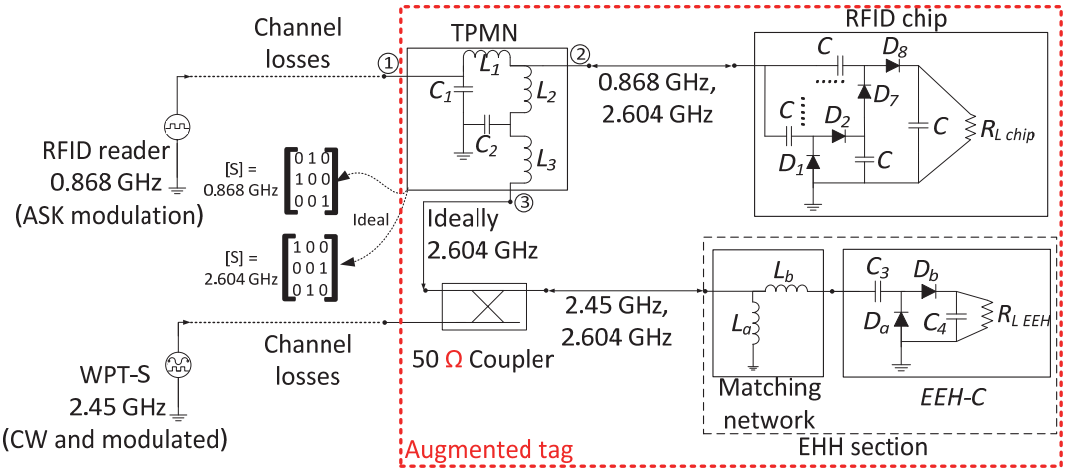

Fig. 1. Schematic of the model used to evaluate the benefits of the nonlinear operation of rectifier devices operating at different frequencies and cohabiting in a single system, i.e., the augmented tag. The RFID reader generates ASK signals and the WPT-S generates CW and signals with different modulations. In a real scenario, the channel losses represent the link budget of an RF communication considering antennas and propagation losses. The model used considers the following component values: RFID chip model C = 1.6 pF, D_1-D_8 = HSMS285, $R_{L\ chip}$ = 34 kΩ; TPMN L_1 = 33 nH, L_2 = 57.4 nH, L_3 = 115.7 nH, C_1 = 0.1 pF, C_2 = 0.1 fF; EEH section L_a = 1 nH, L_b = 3.9 nH, C_3 = 1.2 pF C_4 = 2.7 pF, D_a-D_b= Skyworks SMS7630, $R_{L\ EEH}$ = 5 kΩ.

intervals. Some groups are currently dedicating efforts to study and develop efficient techniques of harvested power-management [22], [23]. The techniques are based in the co-design of harvester and power-management blocks in order to transfer the energy with minimal loss to the energy storage element and to monitor the energy storage and provide charge control and protection for the energy storage used. The deployment of autonomous nodes including operation functions (e.g. identification, moisture or temperature sensing, etc. [24], [25]) is possible thanks to the managing and monitoring of the harvested power. The harvesting approach proposed in this paper may be a candidate to integrate such a managing system.

B. System considerations

The proposed system, so-called augmented tag integrates two sections: (i) the RFID section composed by a passive RFID chip and an RFID reader both operating at 0.868 GHz, and (ii), the Electromagnetic Energy Harvesting (EEH) section composed by an EEH-C and a Wireless Power Transmitter Source (WPT-S) both operating at 2.45 GHz. The schematic of the augmented tag is presented in Fig. 1 and explained below.

- The RFID chip is modeled by a 4 diode-based voltage doubler stages constituting a rectifier circuit with a configuration similar to one used in the Dickson charge pump [26].
- A dual-frequency Three-Port Matching Network (TPMN) is included to interconnect both the different sections in a common system. The TPMN matches the capacitive impedance of the chip in port 2 to the 50 Ω input corresponding to an antenna (at 868 MHz) and to the 50 Ω of the coupler that goes through the EEH-C (at 2.604 GHz). In the dual-frequency multiport operation context, a design trade-off is done in order to achieve the dual band operation of port 2.
- A 50 Ω directional coupler with 10 dB Coupling Factor (CF) is used to combine the $3f_{0chip}$ with the WPT-S signal at the input of the EEH-C. It is worth noting that hereinafter all WPT-S power configurations refer to the power injected by the source before the coupler.
- The 50 Ω EEH-C is composed by a single stage of a voltage doubler and a matching network centered in 2.45 GHz. A first value of $R_{L\ EEH}$ is as the load that allows achieving the higher RF-to-dc conversion. The value is driven by the load input value of the dc input of a RFID EM432 chip where the dc energy could be consumed in an application example [27]. The EEH-C design is similar to the one proposed in [13].
- The RFID reader and the WPT-S are modeled by two 50 Ω RF sources. Simulations consider for both, the RFID reader and the WPT-S, CW signals. Contrary the experimental part considers ASK RFID signals for the reader and different modulations for the WPT-S.
- The propagation losses in a real scenario, in where transmitting and receiving antennas are used are considered by the parameter *channel losses* in Fig. 1.

C. System design methodology

Advanced Design Software (ADS) simulation tools from Keysight are used for the design of each section and its integration to constitute a single system. Three main steps define the design methodology:

- The 1st step is the modeling of the RFID chip. Using the Large-Signal S-Parameters (LSSP) and Harmonic Balance (HB) tools, the RFID chip model is optimized at 0.868 GHz and for -9 dBm input power, considered to be its activation threshold (EM 43235 RFID chip is used). Three main directives leaded the model design: (i) nonlinearity, i.e. harmonic generation and impedance-power dependency should be reproduced; (ii) the model should present a capacitive input impedance comparable to the ones reported in commercial RFID chips [9]; (iii) under power regulations, the model should produce at least 1V of dc required to activate the logic part of the chip [24]. A

first value for R_{LChip} that allows complying with the directives is here selected. The dc management and voltage regulator for high dc levels are out of the scope of this work. Fig. 2 depicts the input impedance of the RFID chip model at its activation threshold; at 0.868 GHz the model presents 11 – j138 Ω as impedance.

- The 2nd step is the TPMN design using the S-parameters tool and considering in first approach the other devices as linear in order to define its topology. The dual-frequency functionality of the TPMN with addition to three impedance matching functions represents the major difficulty for its design. Being the redirection of $3f_{0chip}$ towards the EEH-C the key of the proposed approach, the TPMN design is foremost driven by this priority.
- The 3rd step is the system integration performing the TPMN optimization. This step uses LSSP and HB tools and considers the nonlinearity of the RFID chip and EEH-C. The optimization goal is to satisfy the 1 V requirement at the RFID chip dc output and to maximize the $3f_{0chip}$ level at the EEH-C input. Two limit configurations of the power injected into node 1 of Fig. 1 are defined: $Power_1$ represents the power that allows activating the augmented tag, and $Power_2$ represents the power when the reader transmits the maximum allowed by regulations [28]. Fig. 3 shows the dc output of the RFID in function of the power delivered by the WPT-S and for the two reader power configurations injected into node 1. The 1 V dc voltage need is satisfied and its output does not depends on the WPT-S power, then validating the correct operation of the TPMN.

From the presented methodology, the last optimization step leads to the optimal component values of the system detailed in Fig. 1. Table I presents the reflection coefficient and quality factor Q of the optimized TPMN. The dual band matching trade-off at port 2 presents a slightly diminished reflection coefficient at 868 MHz, i.e., -5.8 dB, prioritizing the one at 2.604 GHz, i.e., -10.4 dB. The diminished matching at 0.868 GHz is enough to activate the chip satisfying the three modeling directives above exposed. From the presented model, the proposed full system in terms of the nonlinear exploitation is in-depth studied in the next section.

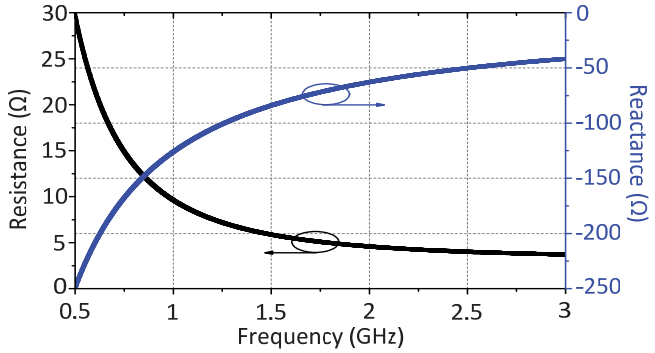

Fig. 2. Input impedance of the RF model for a passive RFID chip. At 0.868 GHz the model has an impedance of 11 – j138 Ω.

TABLE I PERFORMANCE OF THE TPMN.

	Port 1	Port 2	Port 3
@ 0.868 GHz	S_{11} = -12 dB Q = 11.9	S_{22} = -6 dB high Q	-
@ 2.604 GHz	-	S_{22} = -10 dB Q = 325.5	S_{33} = -11 dB Q = 260.4

*The TPMN considers the capacitive impedance of the RFID chip at port 2 and 50 Ω for port 1 and port 3.

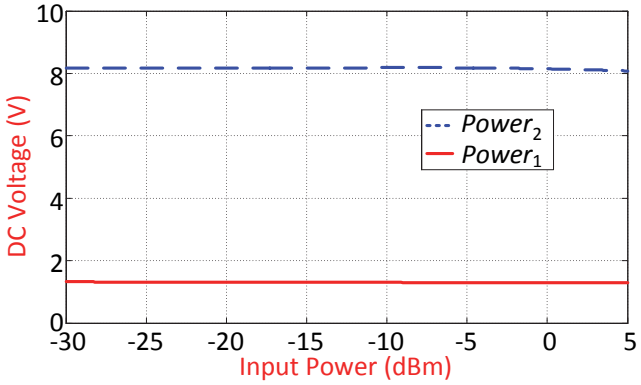

Fig. 3. DC voltage produced by the rectifier part of the RFID chip versus WPT-S power. The values are modeled at two limit powers injected into node 1. In both cases, the requirement of 1 V to feed the logic part of the chip is satisfied.

IV. SIMULATION STUDY

The aim of this section is to highlight and quantify the nonlinear contribution of the cooperative system above modeled. The power matching, multisource operation, $3f_{0chip}$ rectification and its effects on the RF-to-dc conversion efficiency of the EEH-C are notably studied.

A. Contribution of the RFID chip nonlinearity

In order to quantify the nonlinearity introduced by the RFID chip, i.e., the $3f_{0chip}$ level, a linear model of the RFID chip is used as a comparative reference. The linear model, which does not produce any harmonic nor changes its impedance respect to the power, consists of the impedance file of the nonlinear RFID chip model calculated at its activation threshold.

Let assume an RFID reader that communicates with the augmented tag (considering 0 dB tag antenna gain) for 1 m distance between each other (i.e., 31.21 dB of propagation losses at 0.868 GHz). If the augmented tag sensitivity is -9 dBm, the power injected into node 1 of Fig. 1, so-called $Power_1$, should be equal to -9dBm. The maximum power injected into the same node, considering the propagation losses in agreement with the regulations [28] and so-called $Power_2$, would be approximately 5 dBm. Additionally, three WPT-S power configuration cases are defined:

- -6 dBm (case 1) which corresponds to the injected power into the augmented tag by a Wi-Fi router transmitting at its maximum allowed Equivalent Isotropic Radiated Power (EIRP), i.e., 36 dBm at 1 m distance [21];
- -13 dBm (case 2) which corresponds to the injected power into the augmented tag by the same Wi-Fi router distanced 3 meters;

- WPT-S is off (case 3).

Hereinafter the values of $Power_1$, $Power_2$ and the three WPT-S power configurations are kept constant for all the simulation tests.

In order to quantify $3f_{0chip}$ in function of the reader power, the Power Spectral Density (PSD) calculated at the EEH-C input is analyzed at WPT-S = -6 dBm. Fig. 4 and Fig. 5 show the PSD for a linear chip model and for the chip producing harmonics, respectively. Thanks to the HB tool, the analysis of the linear chip allows determining the weak presence of the 3rd harmonic of the RFID reader signal produced by the EEH-C (indeed, the linear chip does not produce harmonics but the EEH-C is always nonlinear). The weak leakage of -35 dBm is only distinguishable for $Power_2$. The analysis of the nonlinear chip model shows a greatly distinguishable $3f_{0chip}$ level: $3f_{0chip}$ reaches -27 dBm with $Power_1$ and more than - 10 dBm with $Power_2$. The rectification of this $3f_{0chip}$ is the aim of the intended multisource operation.

Finally, small variations on the 2.45 GHz signal strength due to the reader power injected into node 1 can be also observed. This phenomenon is studied in detail in subsequent paragraphs.

B. System performance

The key parameter to evaluate the EEH-C performance is the RF-to-dc conversion efficiency (η) defined as the ratio of the dc output power (P_{dc}) by the RF input power into the EEH-C (P_{RF}). Given the multisource operation and the $3f_{0chip}$ exploitation approach, a fair evaluation of the EEH-C needs an accurate definition of η. From the PSD analysis shown in Fig. 5, the RF signals that significantly contribute to P_{RF} are: the power at 0.868 GHz leaked from the reader ($P_{RF@0.868}$), the power at 2.45 GHz coming from the WPT-S ($P_{RF@2.45}$), and the power at 2.604 GHz due to the $3f_{0chip}$ contribution ($P_{RF@2.604}$). The intermodulation products observed in the PSD are very weak and therefore noncontributory to P_{RF}. With these considerations, η of the EEH-C is defined in (1):

$$\eta = \frac{P_{dc}}{P_{RF}} = \frac{P_{dc}}{P_{RF@0.868} + P_{RF@2.45} + P_{RF@2.604}} \quad (1)$$

1) Effects of the reader power in the system

In order to quantify the effect of the reader power and the contribution of $3f_{0chip}$ in the EEH-C performance, Fig. 6 shows η versus the reader power injected into node 1 and for the different WPT-S configurations. Continuous lines represent η with the chip model generating a 3rd harmonic and dash lines represent η with a linear chip model.

The benefit, introduced only by the multisource operation, can be studied with the linear chip model when $3f_{0chip}$ is not present. Looking at Fig. 6 in curves (b) and (d) in where the multisource is set and a linear chip model is considered (i.e. $3f_{0chip}$ does not exist), the EEH-C conversion efficiency is higher respect to curve (f) in where only the reader is active.

The benefit introduced only by the $3f_{0chip}$ rectification can be studied comparing the linear and nonlinear chip models when the WPT-S is off. Looking at Fig. 6 in curve (e) in

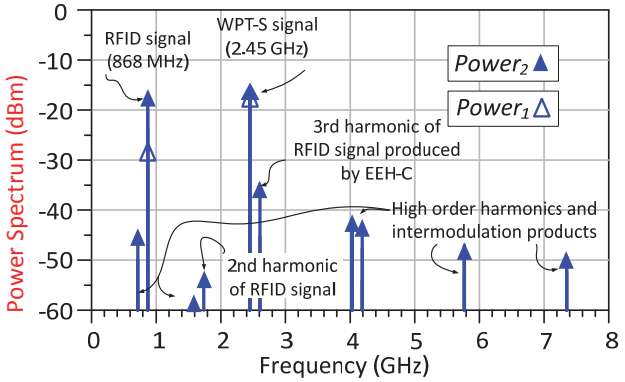

Fig. 4. Power spectral density with linear RFID chip model. The PSD is taken at the input of the EEH section in Fig. 1. There is not generation of harmonics due to the chip but a weak harmonic coming from the reader.

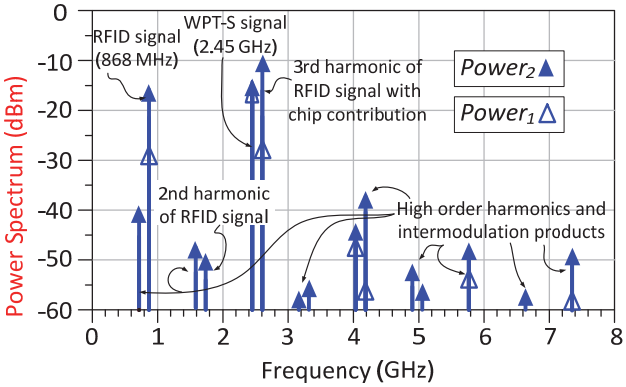

Fig. 5. Power spectral density with nonlinear RFID chip model. The PSD is taken at the input of the EEH section in Fig. 1. The chip generates a 3rd harmonic signal. The reader power slightly affects the signal level at 2.45

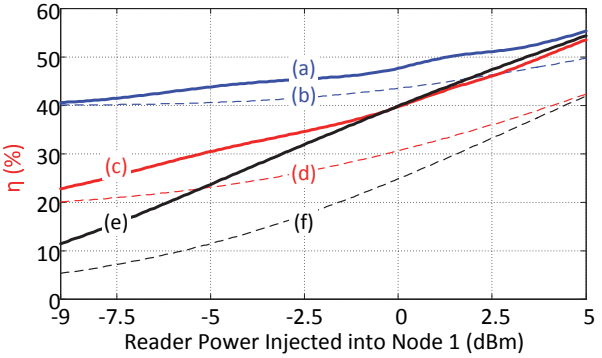

Fig. 6. η versus the power received in node 1 from the reader. Continuous lines represent η with the chip model generating a 3rd harmonic and dash lines represent η with a linear chip model. (a) and (b) Case 1, WPT-S equal to -6 dBm. (c) and (d) Case 2, WPT-S equal to -13 dBm. (e) and (f) Case 3, WPT-S off.

where only the reader transmits and a nonlinear chip model is considered (i.e. $3f_{0chip}$ exists), the EEH-C conversion efficiency is higher respect to curve (f), in where the chip has a linear model. Indeed the $3f_{0chip}$ can be increased, so also η, by increasing the reader power. However at higher levels, due to the saturation behavior of the diode at large signals, η is limited and all curves converge.

2) Effects of the WPT-S power in the system

Besides the contribution of $3f_{0chip}$, the effect of the WPT-S power in the EHH-C conversion performance is studied. Fig. 7 shows η versus the WPT-S power for three power cases: $Power_1$, $Power_2$ and reader off, and for the two chip models

(i.e., linear and nonlinear).

At low WPT-S power, the multisource operation cases (red and blue curves) allows achieving an enhancement of η compared to the single WPT-S case (black curve), especially as high reader power. At high WPT-S power, the greater contributor to η is the WPT-S, due to the optimized design of the EHH-C at 2.45 GHz. Combining both sources, in the best of the cases (blue curve with $Power_2$ in respect to black curve), an RF-to-dc conversion efficiency 55 % greater than the case using only the WPT-S is achieved. As a result, the approach of improving η by means of a multisource operation and $3f_{0chip}$ rectification is demonstrated by simulations.

V. Experimental Evaluation

The aim of this section is to experimentally verify and quantify the nonlinear contribution of the proposed cooperative system considering a commercial RFID passive chip and also more complex WPT-S signals. As discussed in Section II, alternatively a finite bandwidth signal with arbitrary modulation can be expressed mathematically in a general form as a (multi-harmonic) signal with a time-varying envelope. Based on the described concept an emulated prototype is designed, and two kinds of experiments are performed in order to evaluate the RF-to-dc conversion efficiency of the EEH section in function of: (i) the composite signal (Section A); (ii) the WPT-S waveform, i.e., a finite bandwidth signal with arbitrary modulation, (Section B).

The complete setup is shown in Fig. 8. Specific details are below described.

- The RFID section is composed by two parts: (i) the antenna emulator composed by two impedance tuners Microlab SF-30F connected in series to offer a power matching between reader, chip and EHH section; (ii) the RFID chip EM4325 shown in Fig. 8(a) is fixed in a SMA connector [9]; when the matching is achieved, the chip response is detected by the reader.
- The TPMN shown in Fig. 8(b) is emulated by the combination of the impedance tuners with a first 50 Ω directional coupler with Coupling Factor (CF = 25 dB). A trade-off power matching is done by activating the chip while maximizing the $3f_{0chip}$ level at the input of the EEH section.
- A second directional coupler (CF = 25 dB) is used to couple the $3f_{0chip}$ with the WPT-S signal and feed the EEH section.
- The EEH section shown in Fig. 8(c) is the same to the one designed in the simulation study. It is composed by a 50 Ω matching network in series with a single stage of a voltage doubler consisting of two Skyworks SMS7630 Schottkty diodes as in [13]. The dc section at the output consists of a low-pass filter capacitor and a resistor $R_{L\ EEH}$ in where the dc level is measured.
- The Speedway Revolution RFID reader and an external source at 2.45 GHz (Agilent N5182A Vector Signal Generator (VSG)) represents the reader and the WPT-S respectively as above described.
- For power tests, a 50 Ω digital Oscilloscope (Agilent 91204 DSO) is connected instead of the EEH section in order to measure the PSD of the input.

Fig. 7. η versus WPT-S power. Continuous lines represent η with the chip model generating a 3rd harmonic and dash lines represent η with a linear chip model

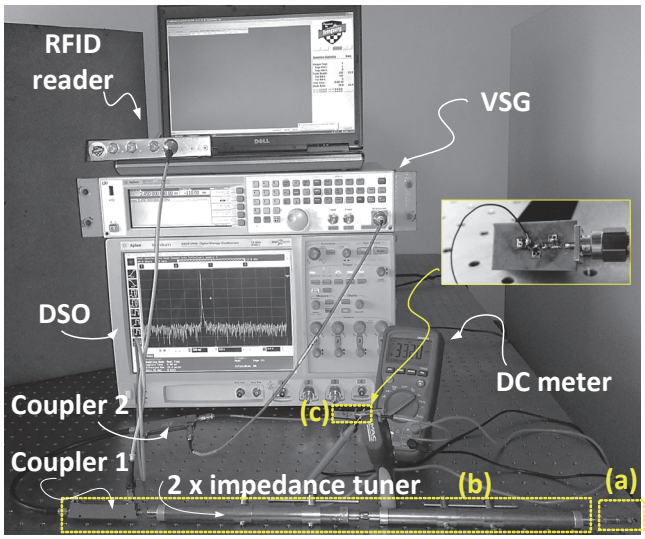

Fig. 8. Measurement setup and emulated prototype. Schematic diagram at the top and implemented setup at the bottom. (a) RFID chip, (b) Three port matching network, (c) EEH section.

Once all sections are integrated, a power matching trade-off is done with the impedance tuners. The principle is to activate the RFID chip (looking for the minimum chip activation threshold in the RFID reader) while maximizing the $3f_{0chip}$ level at the input of the EEH section. The visualization of the PSD in the DSO allows performing this analysis.

Four main differences valorize this experimental evaluation from the reported one in [29]: (i) the reader, that activates the

RFID chip, is always present, and it varies its power; (ii) the losses in the system are reduced due to the use of two directional couplers instead of three; (iii) the dc output of the EHH-C is not connected to the dc input of the chip because of the intention to quantify its value; (iv) a new definition of η presented in Section IV-B, allows evaluating the EEH-C more accurately.

Following the power limits defined in Section IV-A, and considering the described setup, the conducted power of the Speedway Revolution reader that activates the augmented tag is 17.5 dBm, and the maximum one is 31.5 dBm. After calibration, these values represent $Power_1 = -9\ dBm$ and $Power_2 = 5\ dBm$ (subtracting 26.5 dB of losses in the coupled path of Fig. 8 due to the CF and connectivity). Hereinafter the values of $Power_1$ and $Power_2$ are kept constant for all experimental tests. These power settings allow calculating the scaled read range of the augmented tag. Always considering a tag antenna of 0 dB gain and -9 dBm sensitivity, a read range of 4.8 m is estimated in over-the-air configuration complying with the regulations [28], [30]. It is worth noting that the chip sensitivity of the chosen sample, i.e., -9 dBm, is not affected by the system integration, therefore the standard reading range for tags using this kind of chip is respected.

A. Multisource power dependency

This first analysis evaluates η under a multisource operation scenario, i.e., in terms of the power simultaneously emitted by the RFID reader and the WPT-S. Fig. 9 depicts the measured dc output versus the WPT-S power for the two reader power configurations and without reader. Results for $Power_1$ and reader off are quite close each other due to the losses introduced by the emulated TPMN; however the improvement of combining sources is still notable. Moreover, higher dc values are obtained for $Power_2$.

In order to accurately calculate η as in (1), an experimental PSD analysis at the input of the EEH section is necessary. The analysis is possible thanks to the use of the DSO. Fig. 10, comparable with Fig. 5, shows the normalized measured PSD of a multisource configuration (reader and WPT-S) firstly reported in [29]. When both sources are active, the PSD shows measurable values of $P_{RF@0.868}$ (RFID communication signal), $P_{RF@2.45}$ (signal to be harvested), and $P_{RF@2.604}$ ($3f_{0chip}$ to be harvested). Performing the analysis with the setup above described, the experimental calculation of η is possible.

Fig. 11 shows η versus the WPT-S power for both reader configurations and without reader, and compares the results to the ones obtained by simulation at the lowest power. An improvement of 8 % in η can be noted for $Power_2$ at low WPT-S power (blue curve from -30 dBm to -20 dBm) compared to the single WPT-S operation (black curve). As a result, the behavior predicted by simulations in Section IV-B is verified by measurement, i.e., the $3f_{0chip}$ combined with the WPT-S signal triggers in an enhanced η. Even if the magnitudes are less than the simulated ones (comparing simulated and measured cases); the experimental results validate the approach. Magnitude differences from the simulation results have two expected reasons: (i) losses in the emulated prototype (especially the use of a coupler in the TPMN and chip fixture); and (ii), differences in the commercial chip performance compared to the simulated model.

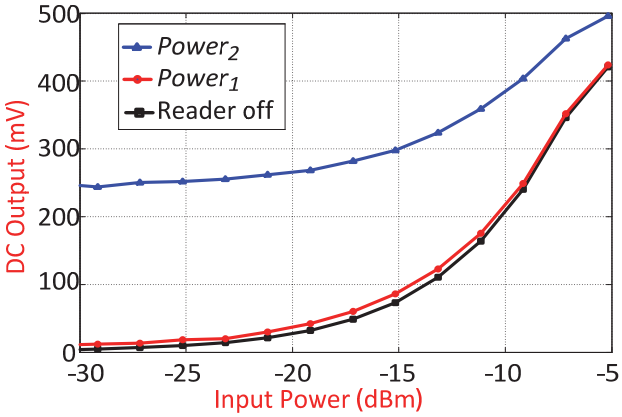

Fig. 9. Harvested dc output in function of the input power at 2.45 GHz. The experiment is performed for the two reader power configurations. Greater values are obtained when the reader transmits its maximum allowed, i.e., $Power_2$.

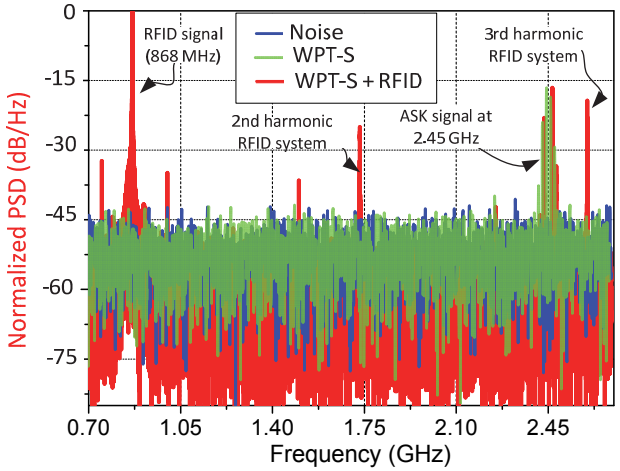

Fig. 10. Normalized power spectral density visualized on the DSO when the sections are interconnected in the setup reported in [19]. When both sources are active, a richest spectrum favors the conversion efficiency of the harvester circuit.

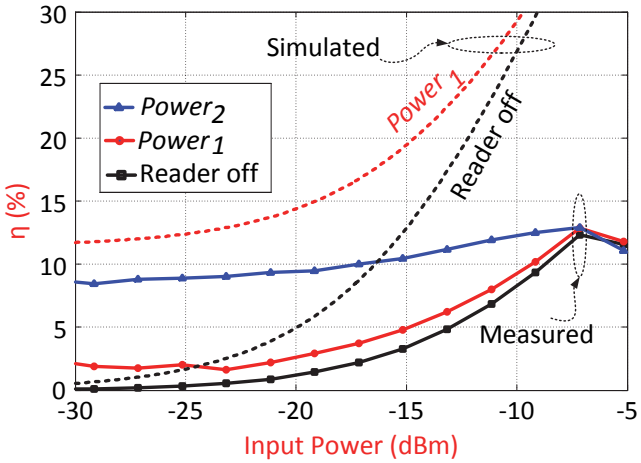

Fig. 11. RF-to-dc conversion efficiency of the EEH-C in function of the input power at 2.45 GHz. In dashed line the simulated values

B. *WPT-S waveforms dependency*

The previous tests have considered the WPT-S transmitting a CW tone. In this part, a time-varying envelope signal generated at the input of the EHH section by the composite signal composed by the tone triggered by the multisource

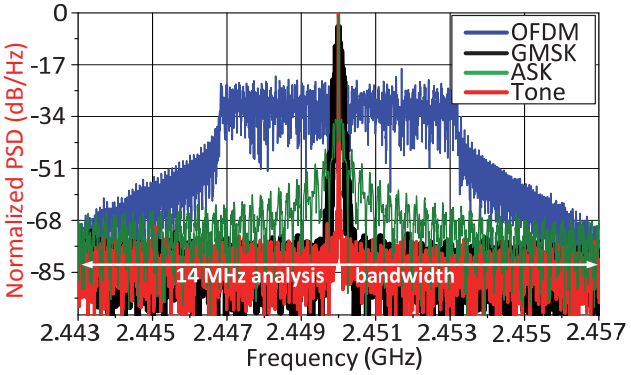

Fig. 12. Normalized power spectral density visualized on the DSO at the EEH input when the sections are interconnected. The average power is the same for all signals. 14 MHz are taking into account for the waveform analysis

operation of the system and the 3rd harmonic RFID product. Hereinafter, and in addition to the composite tone signal approach, the WPT-S signal waveform is configured with the intention to study its effect on EEH section conversion efficiency. It is worth noting that during all tests the RFID reader and chip are communicating.

1) *Studied waveforms and their characteristics*

At the input of the EHH section, four kinds of composite waveforms are studied by combining a modulated signal from the WPT-S with the leaked signal at 0.868 GHz and the redirected $3f_{0chip}$. It is worth noting that the 0.868 GHz and $3f_{0chip}$ signals are from the RFID communication using ASK modulation [28]. In the WPT-S, three modulations commonly used in wireless systems are set, in addition to the CW tone: Orthogonal Frequency-Division Multiplexing (OFDM), Gaussian Minimum-Shift Keying (GMSK), and Amplitude-Shift Keying (ASK).

Fig. 12 shows the normalized PSD of the three modulated and the CW tone above considered. All signals are set with the same average power and centered at 2.45 GHz.

Using a Tektronix RSA5000 Spectrum Analyzer in the position of the DSO in Fig. 8, the Complementary Cumulative Distribution Function (CCDF) of the envelope of the composite waveforms (WPT-S signal plus leaked 0.868 GHz signal and the redirected $3f_{0chip}$) in function of the distance to its average power in dB is measured and results are shown in Fig. 13. This plot gives information about the instantaneous power of the composite time signal. Actually, the value in where the CCDF curve intersects the x-axis indicates the maximum PAPR of the signal envelope; and therefore, the maximum PAPR of the signal can be estimated adding 3 dB to the PAPR of the signal envelope [10]. According to Fig. 13, composite signals using OFDM in the WPT-S have the highest PAPR, followed by the ones using ASK and finally, very close to each other, are the one using GMSK and the CW tone, with PAPR values very close to zero due to the almost null variation of the envelope.

2) *Effect of the waveform in the conversion efficiency*

In order to evaluate η when different waveforms are used to operate the EEH section, the signal power is evaluated as the total average power in 14 MHz bandwidth around the carrier

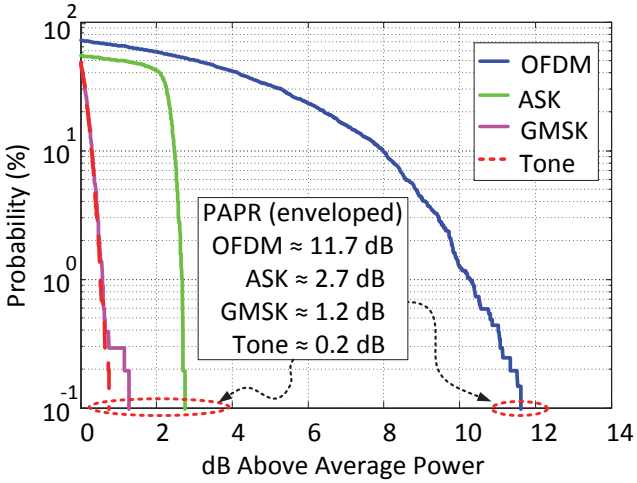

Fig. 13. Measured CCDF of the envelope of the test signals.

TABLE II CONVERSION EFFICIENCY AND HARVESTED POWER IN THE EEH-C LOAD FOR DIFFERENT WAVEFORMS

	TONE		GMSK		ASK		OFDM	
	a	*b*	*a*	*b*	*a*	*b*	*a*	*b*
injected power in node 1= $Power_1$								
η(%)	2.18	14.41	3.74	17.81	0.64	18.98	0.66	23.16
Power (μW)	0.0	24.74	0.02	25.93	0.04	31.89	0.04	40.64
injected power in node 1= $Power_2$								
η(%)	8.56	13.77	9.01	14.33	10.31	14.61	10.91	14.63
Power (μW)	12.00	42.87	12.63	40.86	14.46	44.18	15.28	46.08

*conditions "*a*" and "*b*" represent limit WPT-S average input power equal to -30 dBm and -6 dBm, respectively.

(see in Fig. 12). An accurate evaluation of η should also consider the effect of the reader (the signal level entering to the EEH section at 2.45 GHz is slightly affected by the reader power as seen in Fig. 5), in this context a figure of gain is defined in (2):

$$Efficiency\ gain = 10\log\left(\frac{\eta_{Power_2}}{\eta_{Power_1}}\right) \quad (2)$$

where η_{Power_1} and η_{Power_2} are the conversion efficiency of the EEH-C calculated for $Power_1$ and $Power_2$, respectively.

Measured values of the conversion efficiency and the power harvested in the EEH-C load are unfolded in Table II for the limit power configuration cases, and Fig. 14 depicts the figure of gain for each kind of waveforms.

At low WPT-S ("a" columns in Table II), higher gain is obtained combining an optimum waveform with a high reader signal power, i.e., $Power_2$. At high WPT-S power, i.e., above -13 dBm in Fig. 14. ("b" column in Table II), a negative figure of gain is obtained. This means that in a relative comparison, a higher η is obtained when the WPT-S signals are combined

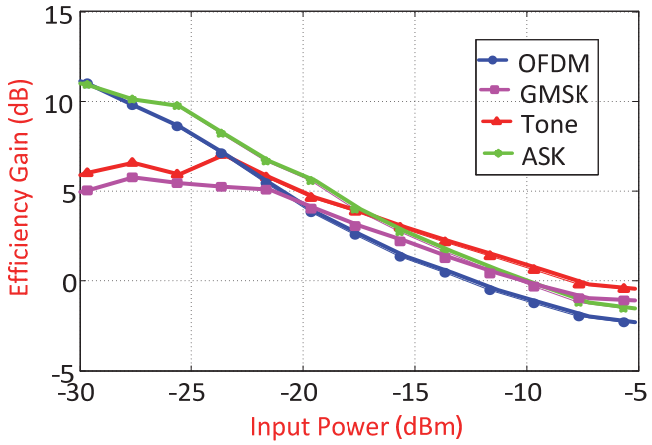

Fig. 14. Figure of gain in the conversion efficiency defined as in (2).

with low power from the reader, i.e., $Power_1$ as depicted in Table II. The same effect is explained in Section IV-B-2 (see Fig. 7) for the case of CW tone.

Reported results show that the waveform can enhance the RF-to-dc conversion efficiency of the EEH-C. Considering the CCDF analysis, OFDM and ASK signals produce higher conversion efficiency because of their higher PAPR compared to GSM and CW signals [10]. The findings of using waveforms with high PAPR in order to increase the conversion efficiency agree with results postulated in the literature [10], [12], [14-19].

VI. Conclusion and Discussion

Nowadays RFID is a well-established technology for identification purposes. Moreover, due to its huge practical advantages such as passive and wireless features, it is more and more considered in order to enable many other applications under the paradigm of Internet of Things. This mainly consists to integrate more of functionalities to the RFID tags such as sensing and localization capabilities. Such an evolution of RFID tag structures requires new additional source of energy and also its optimized management.

This paper proposes and demonstrates the cooperative exploitation of two effects in order to improve the power budget available for augmented passive RFID tags. The first effect is related to the non-linearity of RFID chip that generates wasted power at the 3rd harmonic of fundamental frequency, i.e., 868 MHz in Europe. The second effect lies in the enhancing of the RF-dc conversion efficiency of rectifier circuits by applying multi-frequency excitation signal. Combining the exploitation of these two effects, a unique design is simulated and experimentally emulated. The developed prototype consists of an emulated RFID tag operating at 868 MHz and an Electromagnetic Energy Harvesting circuit operating at the 2.45 GHz ISM band corresponding to existing ambient transmissions, both integrated to operate with a mutual enhanced performance. Moreover, since the composite energy harvesting system exploits the nonlinear i-v characteristic of rectifier circuits using time-varying envelope signals, experiments using different waveforms, i.e. different digitally modulated signals in the 2.45 GHz source are performed. It is worth noting that the emulated prototype has not as objective to reproduce the simulated performances but to validate the exposed concepts using a commercial RFID chip. Three significant results are highlighted:

1) Simulation results based on a simplified chip model show enhancement in the RF-to-dc conversion efficiency when the cooperative operation, considering the RFID chip non-linearity is established. The conversion efficiency rises from 1 % when the 2.45 GHz source transmits at -30 dBm and the RFID reader is off to 56 % when the power injected into the augmented tag at 2.45 GHz (external source) is -30 dBm and the power injected at 0.868 GHz (RFID reader) is 5 dBm.
2) Experimental results also demonstrate an improvement in the RF-to-dc conversion efficiency when the cooperative operation, considering a commercial RFID chip and an emulated prototype, is established. An 8 % enhancement in the conversion efficiency is achieved when the power injected into the tag at 2.45 GHz (using a CW tone) is -30 dBm and the power injected at 0.868 GHz is 5dBm.
3) Experimental results show an RF-to-dc conversion efficiency enhancement using composite signals with high PAPR. The conversion efficiency rises from 14.41 % when the composite system uses a CW signal at 2.45 GHz to 23.16 % when it uses an OFDM signal. In this case the power injected into the tag at 2.45 GHz is -6 dBm and the power injected at 0.868 GHz is equal to the tag sensitivity i.e., -9 dBm and represents 4.8 m of estimated tag read range.

Finally in terms of perspectives, further efforts can be devoted to the use of the cooperative integration milestones exposed in this paper in order to design a single and miniaturized device. Regarding the tag size, a final prototype of the augmented tag may be comparable with current passive RFID tags, e.g. a credit card size using a double face structure integrating an antenna and reducing costs seems feasible [24].

Otherwise, the additional power produced by the cooperative RF harvesting could be profited by low-consumption electronics, e.g., humidity, temperature [24], [25], or air pollution sensors like the CleanSpace-Tag from Drayson-Technologies. Such an enhancement can be also potentially empowered in indoor scenarios where Wi-Fi sources can be seen as hot spots of the application. Furthermore, the read range enhancement can be an option when considerable power is harvested from the additional source (e.g. 2.45 GHz) compensating the propagation losses at 868 MHz.

References

[1] H. Stockman, “Communication by means of reflected power,” Proc. IRE, pp. 1196–1204, Oct. 1948.
[2] A. Rida, L. Yang, M. Tentzeris, “RFID-enabled sensor design and applications,” Norwood, MA: Artech House, 2010.
[3] D. Paret, “RFID at Ultra and Super High Frequencies: Theory and application,” Wiley Publishing, 2010.

[4] L. Yan, Y. Zhang, L. Yang, and H. Ning, "The internet of things: from RFID to the next-generation pervasive networked systems," series: Wireless Networks and Mobile Communications. CRC Press, 2008.
[5] C. Occhiuzzi, G. Marrocco, "Constrained-design of passive UHF RFID sensor antennas," IEEE Trans. Antennas Propag., vol. 61, no. 6, pp. 2972-2980, June 2013.
[6] K. Niotaki, F. Giuppi, A. Georgiadis, A. Collado, "Solar/EM energy harvester for autonomous operation of a monitoring sensor platform," Wireless Power Transfer, vol. 1 no. 01, pp. 44-50, 2014.
[7] C.H.P. Lorenz, S. Hemour, W. Liu, A. Badel, F. Formosa, K. Wu, "Hybrid power harvesting for increased power conversion efficiency," IEEE Microw. Compon. Lett., vol. PP, no. 99, pp.1-1, 2015.
[8] A. Georgiadis, G. Andia Vera, and A. Collado, "Rectenna design and optimization using reciprocity theory and harmonic balance analysis for electromagnetic (EM) energy harvesting," IEEE Antennas Wireless Propag. Lett., vol.9, pp. 444-446, 2010.
[9] G. Andia Vera, Y. Duroc, and S. Tedjini, "Rfid test platform: Nonlinear characterization," IEEE Trans. Instrum. Meas., vol. 63, no. 9, pp. 2299–2305, Sept. 2014.
[10] A. Collado and A. Georgiadis, "Optimal waveforms for efficient wireless power transmission," IEEE Microw. Compon. Lett., vol. 24, no. 5, pp. 354–356, May 2014.
[11] J.A. Hagerty, F.B. Helmbrecht, W.H. McCalpin, R. Zane, Z.B. Popovic, "Recycling ambient microwave energy with broad-band rectenna arrays," IEEE Trans. Microw. Theory Tech., vol. 52, no. 3, pp. 1014-1024, Mar. 2004.
[12] M.S. Trotter, J.D. Griffin, G.D. Durgin, "Power-optimized waveforms for improving the range and reliability of RFID systems, " in Proc. IEEE International Conference on RFID, pp. 80-87, 27-28 Apr. 2009.
[13] G. Andia Vera, A. Georgiadis, A. Collado, S. Via, "Design of a 2.45 GHz rectenna for electromagnetic (EM) energy scavenging, " in Proc. IEEE Radio and Wireless Symposium, pp. 61-64, 10-14 Jan. 2010.
[14] A.S. Boaventura and N. B. Carvalho, "Maximizing dc power in energy harvesting circuits using multi-sine excitation," in Proc. IEEE International Microwave Symposium, Jun. 5–10, 2011.
[15] A. Boaventura, A. Collado, N.B. Carvalho, A. Georgiadis, "Optimum behavior: Wireless power transmission system design through behavioral models and efficient synthesis techniques," IEEE Microwave, vol. 14, no. 2, pp. 26-35, Mar.-Apr. 2013.
[16] C. R. Valenta and G. D. Durgin, "Rectenna performance under power-optimized waveform excitation," in Proc. IEEE International Conference on RFID, pp. 237–244, Apr. 30–May 2 2013.
[17] G. Fukuda, S. Yoshida, Y. Kai, N. Hasegawa, S. Kawasaki, "Evaluation on use of modulated signal for Microwave Power Transmission," in Proc. 44th European Microwave Conference, pp.425-428, 6-9 Oct. 2014.
[18] A. Collado, A. Georgiadis, "Improving wireless power transmission efficiency using chaotic waveforms," in Proc. IEEE International Microwave Symposium, 17-22 June 2012.
[19] D. Belo, N.B. Carvalho, "Behavior of multi-band RF-dc converters in presence of modulated signals for space based wireless sensors," in Proc. in Asia-Pacific Microwave Conference, pp.170,172, 4-7 Nov. 2014.
[20] ETSI, "Electromagnetic compatibility and radio spectrum matters (erm); radio frequency identification equipment operating in the band 865 MHz to 868 MHz with power levels up to 2 W; part 1: technical requirements and methods of measurement," EN 302 208-1 V1.2.1 2008.
[21] IEEE standards association. Part 11: Wireless LAN Medium Access Control (MAC) and Physical Layer (PHY) Specifications [Online]. Available: http://standards.ieee.org/getieee802/download/802.11-2012.pdf
[22] Z. Popovic, S. Korhummel, S. Dunbar, R. Scheeler, A. Dolgov, R. Zane, E. Falkenstein, J. Hagerty, "Scalable RF energy harvesting," IEEE Trans. Microw. Theory Tech., vol. 62, no. 4, pp.1046-1056, April 2014.
[23] A. Dolgov, R. Zane, Z. Popovic, "Power management system for online low power RF energy harvesting optimization," IEEE Trans. Circuits Syst. I, Reg. Papers, vol. 57, no. 7, pp. 1802-1811, July 2010.
[24] V. Palazzi, F. Alimenti, C. Mariotti, M. Virili, G. Orecchini, L. Roselli, P. Mezzanotte, "Demonstration of a high dynamic range chipless RFID sensor in paper substrate based on the harmonic radar concept," in IEEE International Microwave Symposium, 17-22 May 2015.
[25] M. Buettner, R. Prasad, A. Sample, D. Yeager, B. Greenstein, J. Smith, D. Wetherall, "RFID sensor networks with the Intel WISP," in Proc. 6th ACM conference on Embedded Network Sensor Systems, pp. 393-394, Nov. 2008.
[26] G. De Vita, and G. Iannaccone, "Design criteria for the RF section of UHF and microwave passive RFID transponders," IEEE Trans. Microw. Theory Tech., vol. 53, no. 9, pp.2978-2990, Sept. 2005.
[27] G. Andia Vera, S. Nawale, Y. Duroc, and S. Tedjini, "Optimum integration of passive UHF RFID tag-rectenna in a single feed dual band antenna," in Proc. General Assembly and Scientific Symposium, Aug. 2014.
[28] UHF Gen2 Air Interface Protocol, EPC Standard 2.0.1, 2015.
[29] G. Andia Vera, Y. Duroc, and S. Tedjini, "Cooperative integration of harvesting sections for passive RFID communication," in Proc. IEEE International Microwave Symposium, 17-22 May 2015.
[30] K. V. S. Rao, P. Nikitin, S. Lam, "Antenna design for UHF RFID tags: a review and a practical application," IEEE IEEE Trans. Antennas Propag., vol.53, no.12, pp.3870-3876, Dec. 2005.